Long-range interaction and correlation between *MYC* enhancer and oncogenic long noncoding RNA *CARLo-5*

Taewan Kim[a,1], Ri Cui[a,b], Young-Jun Jeon[a], Ji-Hoon Lee[c], Ju Hee Lee[d], Hosung Sim[e], Jong Kook Park[f], Paolo Fadda[a], Esmerina Tili[a,g], Hiroshi Nakanishi[a], Man-Il Huh[h], Sung-Hak Kim[i,j], Ju Hwan Cho[k], Bong Hwan Sung[l], Yong Peng[a], Tae Jin Lee[a], Zhenghua Luo[a], Hui-Lung Sun[a], Huijun Wei[a], Hansjuerg Alder[a], Jeong Su Oh[m], Kang Sup Shim[a], Sang-Bong Ko[n], and Carlo M. Croce[a,2]

[a]Department of Molecular Virology, Immunology and Medical Genetics and [g]Department of Anesthesiology, Wexner Medical Center, and [i]Department of Neurological Surgery, The Ohio State University, Columbus, OH 43210; [b]Department of Pathology, Affiliated Hospital of YanBian University, YanJi 133002, China; [c]Department of Molecular Biology, University of Texas Southwestern Medical Center, Dallas, TX 75235; [d]Department of Applied Mathematics and Statistics, University of California, Santa Cruz, CA 95064; [e]Department of Molecular and Integrative Physiology, University of Michigan Medical School, Ann Arbor, MI 48109; [f]Department of Dermatology, Northwestern University, Chicago, IL 60208; [h]Department of Ophthalmology, School of Medicine, Kyungpook National University, Daegu 700-842, Korea; [j]School of Life Sciences and Biotechnology, Korea University, Seoul 136-702, Korea; [k]Department of Radiation Oncology, The Ohio State University Medical Center, Arthur G. James Comprehensive Cancer Center, Columbus, OH 43210; [l]Department of Cancer Biology, Vanderbilt University Medical Center, Nashville, TN 37232; [m]Department of Genetic Engineering, Sungkyunkwan University, Suwon 110-745, Korea; and [n]Department of Orthopedic Surgery, Daegu Catholic University Medical Center, Catholic University of Daegu School of Medicine, Daegu 705-718, Korea

Contributed by Carlo M. Croce, January 10, 2014 (sent for review December 9, 2013)

The mechanism by which the 8q24 *MYC* enhancer region, including cancer-associated variant rs6983267, increases cancer risk is unknown due to the lack of protein-coding genes at 8q24.21. Here we report the identification of long noncoding RNAs named cancer-associated region long noncoding RNAs (*CARLo*s) in the 8q24 region. The expression of one of the long noncoding RNAs, *CARLo-5*, is significantly correlated with the rs6983267 allele associated with increased cancer susceptibility. We also found the MYC enhancer region physically interacts with the active regulatory region of the *CARLo-5* promoter, suggesting long-range interaction of *MYC* enhancer with the *CARLo-5* promoter regulates *CARLo-5* expression. Finally, we demonstrate that *CARLo-5* has a function in cell-cycle regulation and tumor development. Overall, our data provide a key of the mystery of the 8q24 gene desert.

Several genome-wide association (GWA) studies have reported strong associations between the G allele of rs6983267 at 8q24.21 and increased risk of various types of cancers such as colorectal and prostate cancers (1–3). In addition, a recent in vivo study shows that deletion of the enhancer region, including rs6983267, results in resistance to intestinal tumors (4). Nevertheless, the biological function of rs6983267 remains unclear because the region is located in a gene desert that does not contain protein-coding genes. Several studies have shown that the region including rs6983267 has enhancer activity and interacts with the proto-oncogene *MYC* involved in early steps of colorectal cancer (CRC)–development (5–7). However, no significant correlation between rs6983267 and *MYC* expression was found in humans (5, 8–11).

Long noncoding RNAs (lncRNAs), nonprotein coding transcripts longer than ~200 bp, have recently attracted interest due to their functions in various cellular processes, development, and human diseases (12). For example, Guttman et al. (13) found that a cohort of lncRNAs controls embryonic stem cell state, and Klattenhoff et al. (14) recently revealed that the lncRNA *braveheart* (*Bvht*) has a role in the establishment of cardiovascular lineage, providing the evidence that lncRNAs are involved in embryo development (13, 14). In addition, it was reported that several lncRNAs including *lincRNA-p21* and *PANDA* are implicated in cellular process such as cell growth and apoptosis (15, 16). Several lncRNAs are known to be implicated in tumor development. The lncRNAs such as *HOTAIR*, *lincRNA-HEIH*, and *lincRNA-LALR1* also have a role in tumor initiation or progression (17–19). Thus, the studies of lncRNAs provide keys of the unsolved questions in current scientific knowledge.

Here, we found that the 8q24 gene desert harbors lncRNAs and that the enhancer region including rs6983267 regulates at least one of them by directly interacting with the promoter region of the lncRNA. We also report that the lncRNA has a role in cell-cycle regulation and tumor development.

Results and Discussion

Identification of lncRNAs in the 8q24 Gene Desert. Manual annotation performed by the human and vertebrate analysis and annotation (HAVANA) team discovered putative lncRNAs in the human genome that are available in ENSEMBL. Using this information, we found seven lncRNAs that are located in the 8q24.21 gene desert [hereafter referred to as cancer-associated region long noncoding RNA (*CARLo*; Fig. 1*A*, *Top* and *Middle*)]. To identify and characterize *CARLo*s, we conducted 5′ and 3′ RACE (*Materials and Methods* and Fig. 1*B*). All *CARLo*s and their variants were identified by RACE in CRC-derived cells,

Significance

Many cancer-associated variants have been found in the 8q24.21 region harboring enhancer activity. However, the functional mechanism of the variants is not clear due to the lack of protein-coding genes in the region and no significant correlation with the nearest oncogene *MYC*. We identified long noncoding RNAs (lncRNAs) named cancer-associated region long noncoding RNAs (*CARLo*s) in the 8q24.21 region. Interestingly, we found that the cancer-associated variant rs6983267 regulating the enhancer activity is significantly associated with the expression of one of the lncRNAs *CARLo-5* and that *CARLo-5* has an oncogenic function. By showing direct interaction between the enhancer region and active regulatory region of the *CARLo-5* promoter, we provide a regulatory mechanism of cancer susceptibility caused by the cancer-associated variants.

Author contributions: T.K. and C.M.C. designed research; T.K., R.C., Y.-J.J., H.S., P.F., and H.A. performed research; T.K., J.-H.L., E.T., H.N., Y.P., T.J.L., Z.L., H.-L.S., H.W., J.S.O., K.S.S., and S.-B.K. contributed new reagents/analytic tools; T.K., R.C., Y.-J.J., J.-H.L., J.H.L., J.K.P., M.-I.H., S.-H.K., J.H.C., and B.H.S. analyzed data; and T.K. and C.M.C. wrote the paper.

The authors declare no conflict of interest.

Data deposition: Sequence information of CARLos is available in GenBank (accession nos. JX003864, JX003865, JX003866, JX003867, JX003868, JX003869, JX003870, JX003871, JX003872, JX003873, and JX003874). The raw data of NanoString analysis have been deposited in the Gene Expression Omnibus (GEO), www.ncbi.nlm.nih.gov/geo (accession no. GSE48877).

[1]Present address: Epithelial Biology Center, Department of Medicine, Vanderbilt University Medical Center, Nashville, TN 37232.

[2]To whom correspondence should be addressed. E-mail: carlo.croce@osumc.edu.

This article contains supporting information online at www.pnas.org/lookup/suppl/doi:10.1073/pnas.1400350111/-/DCSupplemental.

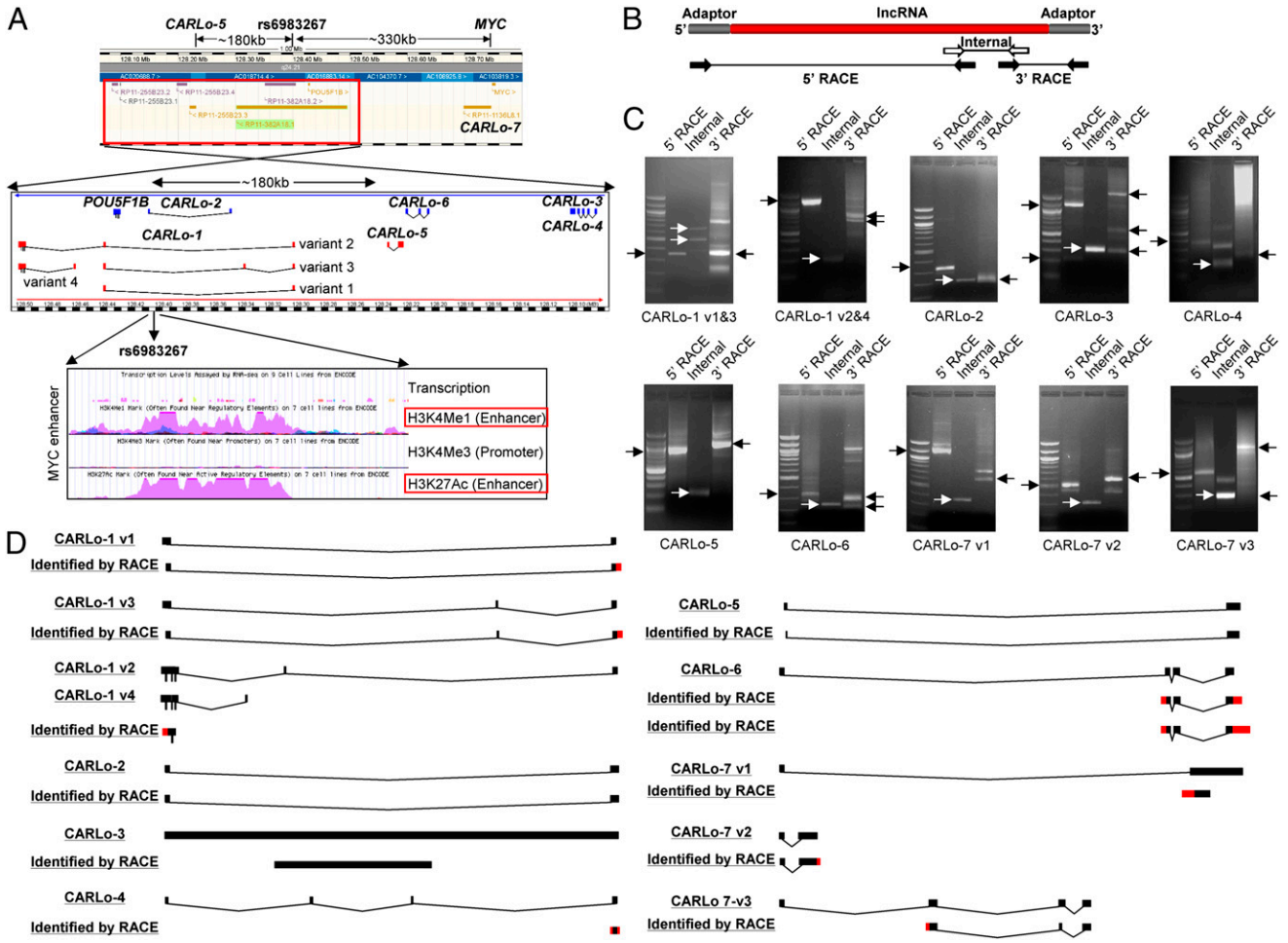

Fig. 1. Identification of lncRNAs in the 8q24 gene desert. (*A*) Schematic view of the 8q24.21 region showing lncRNAs (*CARLo*s) manually annotated by HAVANA. The region including *CARLo-1*~*6* in the *Top* is symmetrically rotated in the *Middle*. (*Bottom*) ENCODE regulation data in the region including rs6983267. The markers representing regulatory (enhancer) activity are highlighted with red-colored boxes. (*B*) Schematic view of RACE strategy. The internal region covers both starting points of 5′ and 3′ RACE. (*C*) The 5′ (*Left* lane) and 3′ (*Right* lane) RACE and amplification of the internal region (*Middle* lane) covering both starting points of 5′ and 3′ RACE. Black arrows indicate appropriate 5′ or 3′ RACE products, and white arrows indicate PCR products of the internal regions. The appropriate PCR products were identified by direct sequencing. (*D*) Schematic view of *CARLo*s predicted by HAVANA (*Upper*) and identified by RACE and direct sequencing (*Lower*). The regions in red indicate additional sequence identified by RACE.

and their actual sequences were determined by direct sequencing (Fig. 1 *C* and *D*). Our findings of lncRNAs demonstrate that the 8q24 gene desert is a gene desert for protein-coding genes, but not for loci-encoding noncoding RNAs including lncRNAs.

It was known that the region including rs6983267 has enhancer activity (5). Using the Encyclopedia of DNA Elements (ENCODE) regulation database available in the University of California Santa Cruz genome browser, we found that markers of regulatory elements such as H3K4Me1 (20) and H3K27Ac (21) are detected at high levels in the region including rs6983267 (Fig. 1*A*, *Bottom*). On the other hand, promoter marker H3K4Me3 (22) and transcripts are not significantly detected in the region, supporting the previous findings (5). Taken together, these data indicate that the region including rs6983267 has enhancer activity rather than gene-coding activity. Based on the evidence, we hypothesized that the rs6983267 region with enhancer activity regulates expression of adjacent noncoding RNAs including *CARLo*s.

Correlation Between *CARLo-5* Expression and rs6983267 in the *MYC* Enhancer Region. To determine whether the *MYC* enhancer region including rs6983267 is involved in the regulation of *CARLo*s, we tested expression levels of *CARLo*s in normal colon tissues classified by alleles of rs6983267. Interestingly, of seven *CARLo*s, the expression level of *CARLo-5* is significantly induced in the tissues with heterozygous [guanine (G)/thymine (T)] or homozygous (G) cancer risk allele of rs6983267 (Fig. 2 *A* and *B*). These results strongly suggest that the rs6983267 region with enhancer activity is implicated in *CARLo-5* regulation. The ENCODE transcription factor binding database shows that TCF4 (TCF7L2) significantly binds to the promoter region of *CARLo-5* in various cancer-derived cells such as HCT116, HepG2, HeLa, and MCF7 (Fig. 3*A*, *Upper*). Using various prediction programs of transcription factor binding, however, we found that there is no predicted sequence for TCF4 binding in the *CARLo-5* promoter region (data not shown). Interestingly, it was reported that the enhancer region including rs6983267 binds with TCF4 (TCF7L2), and the region has a different affinity to the transcription factor TCF4 (TCF7L2) by the different alleles of rs6983267 (8). These results suggest that the 8q24 enhancer region including rs6983267 regulates the expression of *CARLo-5* through long-range interaction with the promoter of *CARLo-5*.

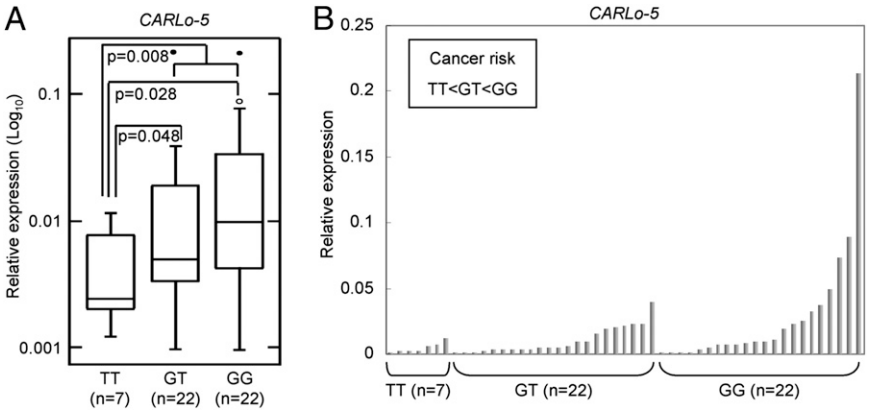

Fig. 2. Correlation between *CARLo-5* expression level and cancer-associated variant rs6983267. (*A*) Box-and-whisker plot showing differential expression levels of *CARLo-5* in normal colon tissues classified by alleles of cancer-associated variant rs6983267. (*B*) Relative expression level of *CARLo-5* in individual normal colon tissue determined by qRT-PCR.

Physical Interaction Between the *CARLo-5* Promoter and the 8q24 Enhancer Region. The enhancer region showed long-range interaction with *MYC* (~335 kb from the region) (5, 23), suggesting that the enhancer region could regulate *CARLo-5* (~180 kb from the region) expression by enhancing its transcription through direct interaction. To test this possibility, we performed chromosome conformation capture (3C) analysis using genomic DNA from CRC-derived HCT116 and RKO cells (*Materials and Methods* and Fig. 3*A*). The results of 3C analysis show that the enhancer region physically interacts with *CARLo-5* (2, 4, 6, 7, 8, and 9 regions generated by HindIII digestion) (Fig. 3 *B* and *C* and Fig. S1).

The physical interaction with the enhancer region was especially found in the active regulatory promoter region (4, 6, and 7 regions generated by HindIII digestion) where the makers of promoter H3K4Me3 (22) and regulatory elements H3K4Me1 (20) and H3K27Ac (21) are highly detected (Fig. 3*A*, *Lower*). These results demonstrate that the enhancer region may regulate expression of *CARLo-5* by direct interaction with the active regulatory 5′ promoter region of *CARLo-5* (Fig. 3*D*). These results suggest that the cancer-associated variant rs6983267 in *MYC* enhancer could regulate *CARLo-5* expression through long-range interaction with the active regulatory region of its promoter.

***CARLo-5* Has a Role in Cell-Cycle Regulation and Tumor Development in CRC.** The genomic region containing *MYC* enhancer is strongly associated with tumor pathogenesis (1–3). In addition, deletion of the enhancer region represses intestinal tumors, supporting the tumorigenic function of the region in animal models (4). Although our results show the involvement of the *MYC* enhancer in *CARLo-5* regulation, no evidence of *CARLo-5* function in tumor development has been elucidated. To determine the

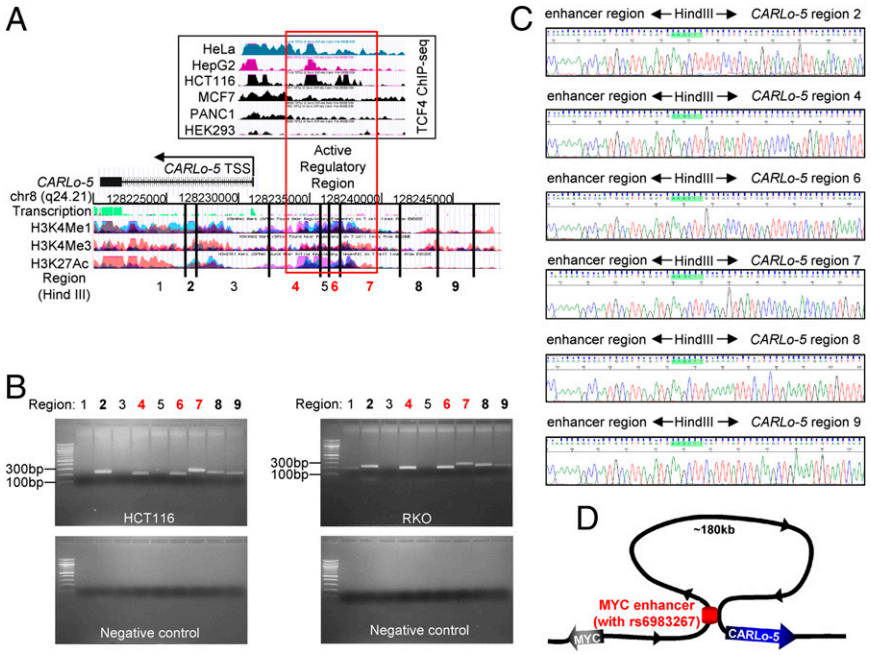

Fig. 3. The 8q24 enhancer region (*MYC* enhancer) physically interacts with the active regulatory region of the *CARLo-5* promoter. (*A*) (*Upper*) TCF4 (TCF7L2) binding in the *CARLo-5* promoter region. (*Lower*) Schematic view of the *CARLo-5* promoter with genomic and epigenetic information. ENCODE gene regulation database showing the active regulatory region in the *CARLo-5* promoter region. The regions generated with HindIII digestion are numbered. (*B*) Direct physical interaction of the active regulatory region of the *CARLo-5* promoter with *MYC* enhancer. The regions that interact with *MYC* enhancer are indicated in bold. The promoter regions with regulatory activity that interact with *MYC* enhancer are indicated in red. The gel images show the ligation bands generated by 3C analysis. No band is seen in the negative control samples without ligase. (*C*) Sequence verification of ligation bands of 3C analysis using HCT116 cells. (*D*) Schematic view of the interaction between *MYC* enhancer and the *CARLo-5* promoter.

function of *CARLo-5*, we investigated the effect of *CARLo-5* in cell proliferation by using *CARLo-5* siRNAs (Fig. 4*A*). Knockdown of *CARLo-5* resulted in decreased proliferation of the various colon-derived cells (Fig. 4*B* and Fig. S2 *A–C*) and increased cell population in the G1 phase (Fig. 4*C*). These results indicate that *CARLo-5* induces cell proliferation by inhibiting G1 arrest.

To identify genes involved in *CARLo-5*–mediated cell-cycle regulation, we used the nCounter Virtual Cell Cycle Gene Sets of the NanoString Gene Expression Assay covering 183 cell-cycle–related genes. By profiling cells treated with siRNA targeting *CARLo-5* (more than 1.5-fold change, P value < 0.05), we detected 24 down-regulated genes and 14 up-regulated genes of the 183 cell-cycle–related genes (Fig. 4*D* and Table S1). By using qRT-PCR, we further confirmed that knockdown of *CARLo-5* increases *CDKN1A* mRNA levels which is a critical regulator of G1 arrest (Fig. 4*E* and Fig. S3).

To further investigate the function of *CARLo-5* in CRC pathogenesis, we measured and compared expression levels of *CARLo-5* in colon-derived cell lines and colon tissue samples. As shown, *CARLo-5* is highly expressed in CRC-derived cell lines compared with normal colon-derived fibroblasts (Fig. 5*A*) and CRC primary tissues compared with their matched normal adjacent tissues (NATs) (Fig. 5*B*). In addition, *CARLo-5* is highly expressed in prostate cancer (PC) tissues compared with their NATs (Fig. S4). These results suggest a putative role of *CARLo-5* in tumor pathogenesis.

To investigate the role of *CARLo-5* in tumor pathology, we tested the function of *CARLo-5* in cell transformation using soft agar colony formation assay and in vivo by xenograft experiments (*Materials and Methods*). Inhibition of *CARLo-5* dramatically reduced the number of cells and colonies in vitro, indicating a role of *CARLo-5* in cell transformation (Fig. 5*C*). Consistently, tumor incidence by xenograft of CRC-derived HCT116 and RKO

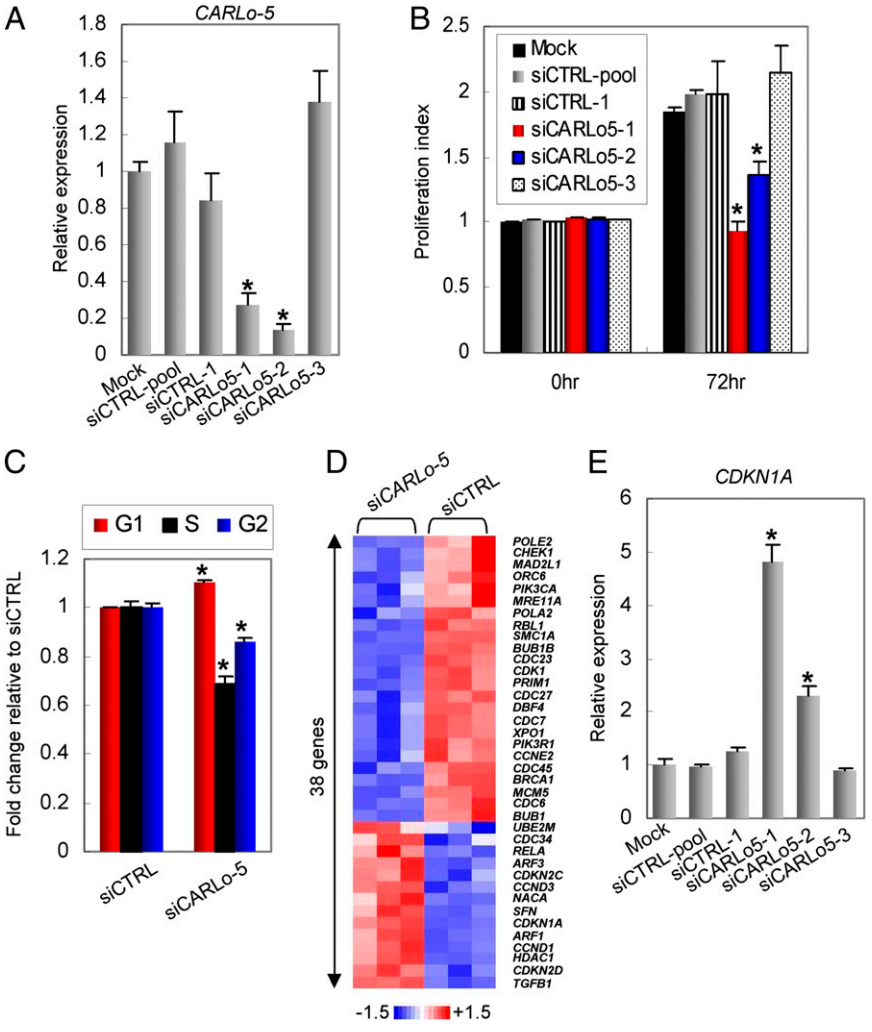

Fig. 4. Function of *CARLo-5* in cell proliferation through cell-cycle regulation. (*A*) Confirmation of the effect of siRNAs targeting CARLo-5 in HCT116 cells using qRT-PCR. The siRNA-1 & 2, but not siRNA-3, for CARLo-5 effectively depletes the expression level of CARLo-5. Mock; no siRNA treated, siCTRL; nontargeting control siRNA pool, siCTRL-1; nontargeting control siRNA. Data are mean ± SD of three independent experiments, each measured in triplicate (*$P \leq 0.01$). (*B*) Cell proliferation assay showing that inhibition of CARLo-5 expression decreases the cell proliferation rate in HCT116 cells. Mock; no siRNA treated, siCTRL; nontargeting control siRNA pool, siCTRL-1; nontargeting control siRNA. Data are mean ± SD of three independent experiments, each measured in triplicate (*$P \leq 0.01$). (*C*) Relative proportion of cell population of each cell-cycle phase in HCT116 cells treated with indicated siRNA. Data are mean ± SD of three independent experiments, each measured in triplicate (*$P \leq 0.01$). (*D*) Heatmap from NanoString gene expression assay representing cell-cycle–related genes dysregulated by knockdown of CARLo-5 in HCT116 cells. Expression values displayed in a gradient of red and blue are Log2-transformed fold change. (*E*) Induction of *CDKN1A* mRNA level by CARLo-5 knockdown in HCT116 cells. Data are mean ± SD of three independent experiments, each measured in triplicate (*$P \leq 0.01$).

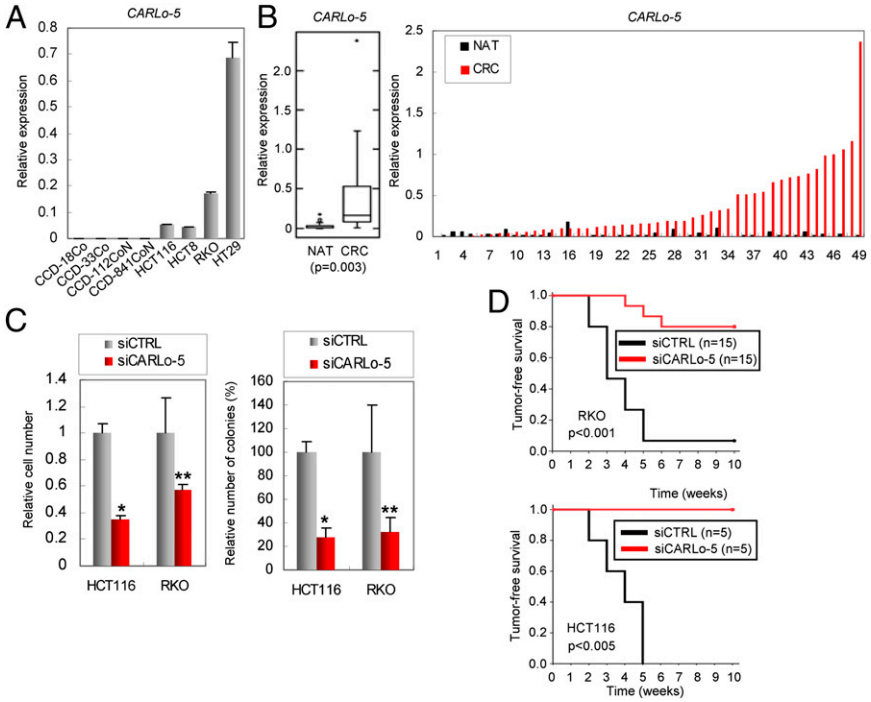

Fig. 5. *CARLo-5* is overexpressed in CRC and involved in oncogenic transformation and tumor incidence. (*A*) Relative expression level of *CARLo-5* in normal colon-derived fibroblast and CRC-derived cell lines. (*B*) Relative expression level of *CARLo-5* in CRC tissues ($n = 49$) and their matched NAT. (*Left*) Box-and-whisker plot showing the significant overexpression of *CARLo-5* in CRC, compared with their matched NAT. (*Right*) Comparison of expression levels of *CARLo-5* in each pair of CRC tissues (red) and their NAT (black). (*C*) Soft agar colony formation assay indicating that knockdown of *CARLo-5* causes a decreased number of cells (*Left*) and colonies (*Right*) in CRC-derived cells. Data are mean ± SD of three independent experiments, each measured in triplicate (**$P \leq 0.05$; *$P \leq 0.01$). (*D*) Kaplan–Meier plot of tumor-free survival analysis in athymic nude mice xenografted with siRNA-treated RKO (*Upper*) or HCT116 (*Lower*) as indicated.

cells was also significantly suppressed by *CARLo-5* inhibition, supporting that *CARLo-5* is not only overexpressed in tumors but also involved in tumorigenesis (Fig. 5*D*).

Because the long-range interaction between *MYC* and the 8q24 *MYC* enhancer was reported, the studies for finding the relationship between *MYC* expression and cancer-associated variants have been done (5, 6). Nevertheless, the clear correlation has not been shown between *MYC* expression and the variants (8, 10). In addition, a recent study reporting the importance of the *MYC* enhancer region in CRC development also failed to show the clear relationship between *MYC* expression and the *MYC* enhancer (4). This contradiction remains in doubt if *MYC* is really implicated in the function of cancer-associated variants in cancer susceptibility. Our findings demonstrate a strong connection between the cancer-associated variant rs6983267 in *MYC* enhancer and *CARLo-5* expression. The physical interaction between the *MYC* enhancer and the active regulatory region of the *CARLo-5* promoter provides strong evidence of the mechanism of the association.

It was recently reported that lncRNA named *CCAT2* are expressed in the *MYC* enhancer region and that *CCAT2* is involved in metastatic progression and chromosome instability of CRC (24). The findings also indicate that lncRNAs are involved in the relationship between 8q24 variants and cancer susceptibility. Although further studies are required to reveal the relationship between *CCAT2* and *CARLo-5*, our findings provide a critical clue of the mystery of 8q24 in cancer susceptibility.

We also show that lncRNAs are transcribed in the 8q24 gene desert and that one of the lncRNAs, *CARLo-5*, has a regulatory role in cell cycle and an oncogenic function with elevated expression in tumors. These results suggest that *CARLo-5* could be a potential target of cancer therapy and that further studies to identify other noncoding RNAs in the gene desert would be helpful to understand the mechanism of how cancer-associated variants can be implicated in cancer susceptibility. Overall, we propose an insight on the function of the 8q24 cancer-associated variants in cancer susceptibility and an approach in the study of disease-related genetic variants in gene deserts.

Materials and Methods

Patients and Primary Colorectal and Prostate Tissue Samples. Primary colorectal and prostate tissue samples were provided by the Department of Pathology, The Ohio State University. All human tissues were obtained according to a protocol approved by the Ohio State Institutional Review Board. Tissue samples were fresh-frozen in liquid nitrogen after surgery and kept at −80 °C. Frozen tissue samples were homogenized using the Tissue Ruptor (QIAGEN) before RNA extraction. Total RNA and genomic DNA were extracted using TRIzol (Invitrogen) in accordance with manufacturer's instructions.

RACE and PCR. The 5′ and 3′ RACE were performed using the SMARTer RACE cDNA Amplification Kit (Clontech). All procedures were done in accordance with manufacturer's instructions. Total RNA from HT29 and SW620 were used. All primers used for RACE, nested PCR, and PCR are presented in Table S2.

Chromosome Conformation Capture Analysis. The 3C library preparation from HCT116 and RKO cells was performed as described before (25). The restriction enzyme HindIII was used for the analysis. The physical interaction between *MYC* enhancer and the *CARLo-5* promoter was tested using PCR and direct sequencing of the PCR products. The primers used in the PCR are described in Table S2.

Quantitative Real-Time–PCR. Total RNA was prepared from cells using TRIZOL (Invitrogen) in accordance with manufacturer's instructions. Total RNA was subjected to Quantitative Real-Time (qRT)– PCR. RNA levels were analyzed using the TaqMan Gene Expression Assays, in accordance with manufacturer's

instructions (Life Technologies). All RT reactions, including no-template controls and RT minus controls, were run in a GeneAmp PCR 9700 Thermocycler (Life Technologies). RNA concentrations were determined with a NanoDrop 20000 (Thermo Fisher Scientific, Inc.). Samples were normalized to GAPDH or OAZ1 for mRNAs and lncRNAs (Life Technologies). Gene expression levels were quantified using the ABI Prism 7900HT Sequence detection system (Life Technologies). Comparative real-time PCR was performed in triplicate, including no-template controls. Relative expression was calculated using the comparative Ct method. Taqman assay for CARLo-5 (Taqman assay ID: AJHSNV9) was designed using a custom assay design tool (Life Technologies), based on sequence information identified by RACE.

Cells, Oligonucleotides, Plasmids, and Transfection. All cell lines were cultured as recommended by ATCC. Custom siRNAs for CARLo-5 were designed by the Dharmacon custom siRNA design tool based on the sequence information identified by RACE. The sequence of the custom siRNAs is described below. As a negative control, smartpool ON-TARGETplus negative control (CTRL) siRNA (mixture of four negative control siRNAs, siCTRL-pool) and ON-TARGETplus Nontargeting siRNA #1 (siCTRL-1) were used. As a mock test, transfection mixture without siRNA was used. Transfection was performed with Lipofectamine RNAiMAx (Invitrogen) in accordance with manufacturer's instructions, and siRNAs were used at 50 nM final concentration.

CARLo-5 siRNA-1 (siCARLo5-1): GGAGGGUGCUUGACAAUAAUU

CARLo-5 siRNA-2 (siCARLo5-2): GAGAAGACCAUAAGAAGAU

CARLo-5 siRNA-3 (siCARLo5-3): UGGGAAAGGUGCCGAGACA

Cell Proliferation Assay. For cell proliferation assay, MTS assay from Promega (CellTiter 96 AQueous One Solution Cell Proliferation Assay) was used following manufacturer's instructions. Briefly, cells in 96-well plates were incubated for 72 or 96 h in humidified 5% (vol/vol) CO_2 atmosphere after transfection with indicated siRNAs, followed by addition of 20 μL CellTiter 96 AQueous One Solution and 1–4 h incubation in humidified 5% (vol/vol) CO_2 atmosphere.

Soft Agar Colony Formation Assay. Soft agar colony formation assay was performed with CytoSelect cell transformation assay (Cell Biolab, Inc.) in accordance with manufacturer's instructions. The cells transfected with the indicated siRNA were incubated for 24 h followed by soft agar colony formation assay.

Xenograft and Tumor-Free Survival Analysis. Animal experiments were approved by The Ohio State University animal care and use committee and conducted following The Ohio State University animal policy in accordance with National Institutes of Health guidelines. The 0.5 million cells (HCT116 and RKO) transfected with indicated siRNAs 24 h before injection were s.c. injected into the right flanks of a 5-wk–old female athymic nude mouse (Jackson Laboratory). Tumor initiation was observed and counted when a palpable tumor (~50–60 mm^3) formed. Tumor volume was determined by measuring the length and the width of the tumor mass and calculating the volume [volume = $(width)^2(length)/2$]. The palpable mass was observed until the volume reaches 100 mm^3 to verify that the palpable mass is a tumor mass. The parental RKO and HCT116 cells that were not transfected with siRNA were also injected, and the results of tumor-free survival with parental cells showed similar results with control siRNA-transfected cells. All athymic nude mice developed palpable tumors 5 wk after injection with the parental cells.

Flow Cytometry Analysis. For DNA content analysis, cells were fixed in methanol at −20 °C, washed again, rehydrated, resuspended in PBS containing 2 μg/mL propidium iodide (PI) and 5 μg/mL RNase A, and analyzed by BD FACS Calibur Flow Cytometer.

NanoString Gene Expression Assay and Data Analysis. For NanoString Gene expression assay analyses, the nCounter Virtual Cell Cycle Gene Set was used, following manufacturer's instructions (NanoString Technologies). Briefly, total RNA (100 ng) were used as input for nCounter mRNA sample preparation reactions. All sample preparation was performed according to manufacturer's instructions (NanoString Technologies). Hybridization reactions were performed according to manufacturer's instructions with 5 μL of the fivefold diluted sample preparation reaction. All hybridization reactions were incubated at 64 °C for a minimum of 18 h. Hybridized probes were purified and counted on the nCounter Prep Station and Digital Analyzer (NanoString Technologies) following manufacturer's instructions. For each assay, a high-density scan (600 fields of view) was performed. Data analysis was performed using the nSolver analysis software (NanoString Technologies) and dChip software.

Statistics. All graph values represent means ± SD from three independent experiments with each measured in triplicate. The differences between two groups were analyzed with unpaired two-tailed Student *t* test. $P < 0.05$ was considered statistically significant and indicated with asterisks as described in the figure legends.

ACKNOWLEDGMENTS. We thank Dr. Thomas D. Schmittgen (The Ohio State University) for the revision of this manuscript. We also thank the human and vertebrate analysis and annotation team for use of the genome annotation database and the Encyclopedia of DNA Elements (ENCODE) consortium for use of the ENCODE regulation database.

1. Yeager M, et al. (2007) Genome-wide association study of prostate cancer identifies a second risk locus at 8q24. *Nat Genet* 39(5):645–649.
2. Haiman CA, et al. (2007) A common genetic risk factor for colorectal and prostate cancer. *Nat Genet* 39(8):954–956.
3. Tomlinson I, et al. (2007) A genome-wide association scan of tag SNPs identifies a susceptibility variant for colorectal cancer at 8q24.21. *Nat Genet* 39(8):984–988.
4. Sur IK, et al. (2012) Mice lacking a Myc enhancer that includes human SNP rs6983267 are resistant to intestinal tumors. *Science* 338(6112):1360–1363.
5. Pomerantz MM, et al. (2009) The 8q24 cancer risk variant rs6983267 shows long-range interaction with MYC in colorectal cancer. *Nat Genet* 41(8):882–884.
6. Ahmadiyeh N, et al. (2010) 8q24 prostate, breast, and colon cancer risk loci show tissue-specific long-range interaction with MYC. *Proc Natl Acad Sci USA* 107(21): 9742–9746.
7. Sansom OJ, et al. (2007) Myc deletion rescues Apc deficiency in the small intestine. *Nature* 446(7136):676–679.
8. Tuupanen S, et al. (2009) The common colorectal cancer predisposition SNP rs6983267 at chromosome 8q24 confers potential to enhanced Wnt signaling. *Nat Genet* 41(8): 885–890.
9. Zanke BW, et al. (2007) Genome-wide association scan identifies a colorectal cancer susceptibility locus on chromosome 8q24. *Nat Genet* 39(8):989–994.
10. Prokunina-Olsson L, Hall JL (2009) No effect of cancer-associated SNP rs6983267 in the 8q24 region on co-expression of MYC and TCF7L2 in normal colon tissue. *Mol Cancer* 8:96–100.
11. Pomerantz MM, et al. (2009) Evaluation of the 8q24 prostate cancer risk locus and MYC expression. *Cancer Res* 69(13):5568–5574.
12. Wapinski O, Chang HY (2011) Long noncoding RNAs and human disease. *Trends Cell Biol* 21(6):354–361.
13. Guttman M, et al. (2011) lincRNAs act in the circuitry controlling pluripotency and differentiation. *Nature* 477(7364):295–300.
14. Klattenhoff CA, et al. (2013) Braveheart, a long noncoding RNA required for cardiovascular lineage commitment. *Cell* 152(3):570–583.
15. Hung T, et al. (2011) Extensive and coordinated transcription of noncoding RNAs within cell-cycle promoters. *Nat Genet* 43(7):621–629.
16. Huarte M, et al. (2010) A large intergenic noncoding RNA induced by p53 mediates global gene repression in the p53 response. *Cell* 142(3):409–419.
17. Gupta RA, et al. (2010) Long non-coding RNA HOTAIR reprograms chromatin state to promote cancer metastasis. *Nature* 464(7291):1071–1076.
18. Yang F, et al. (2011) Long noncoding RNA high expression in hepatocellular carcinoma facilitates tumor growth through enhancer of zeste homolog 2 in humans. *Hepatology* 54(5):1679–1689.
19. Xu D, et al. (2013) Long noncoding RNAs associated with liver regeneration 1 accelerates hepatocyte proliferation during liver regeneration by activating Wnt/β-catenin signaling. *Hepatology* 58(2):739–751.
20. Heintzman ND, et al. (2009) Histone modifications at human enhancers reflect global cell-type-specific gene expression. *Nature* 459(7243):108–112.
21. Creyghton MP, et al. (2010) Histone H3K27ac separates active from poised enhancers and predicts developmental state. *Proc Natl Acad Sci USA* 107(50): 21931–21936.
22. Barski A, et al. (2007) High-resolution profiling of histone methylations in the human genome. *Cell* 129(4):823–837.
23. Sotelo J, et al. (2010) Long-range enhancers on 8q24 regulate c-Myc. *Proc Natl Acad Sci USA* 107(7):3001–3005.
24. Ling H, et al. (2013) CCAT2, a novel noncoding RNA mapping to 8q24, underlies metastatic progression and chromosomal instability in colon cancer. *Genome Res* 23(9):1446–1461.
25. Hagège H, et al. (2007) Quantitative analysis of chromosome conformation capture assays (3C-qPCR). *Nat Protoc* 2(7):1722–1733.